

Interaction between the Water Soluble Poly{1,4-phenylene-[9,9-bis(4-phenoxy butylsulfonate)]fluorene-2,7-diyl} Copolymer and Ionic Surfactants Followed by Spectroscopic and Conductivity Measurements

M. J. Tapia,^{*,†} H. D. Burrows,^{*,‡} A. J. M. Valente,[‡] S. Pradhan,[§] U. Scherf,[§] V. M. M. Lobo,[‡] J. Pina,[‡] and J. Seixas de Melo[‡]

Departamento de Química, Universidade de Coimbra, 3004-535 Coimbra, Portugal, Departamento de Química, Universidad de Burgos, Plaza Misael Bañuelos s/n, Burgos 09001, Spain, and Makromolekulare Chemie, Bergische Universität Wuppertal, D-42097 Wuppertal, Germany

Received: April 29, 2005; In Final Form: July 21, 2005

The interaction has been studied in aqueous solutions between a negatively charged conjugated polyelectrolyte poly{1,4-phenylene-[9,9-bis(4-phenoxybutylsulfonate)]fluorene-2,7-diyl} copolymer (PBS-PFP) and several cationic tetraalkylammonium surfactants with different structures (alkyl chain length, counterion, or double alkyl chain), with tetramethylammonium cations and with the anionic surfactant sodium dodecyl sulfate (SDS) by electronic absorption and emission spectroscopy and by conductivity measurements. The results are compared with those previously obtained on the interaction of the same polymer with the nonionic surfactant C₁₂E₅. The nature of the electrostatic or hydrophobic polymer–surfactant interactions leads to very different behavior. The polymer induces the aggregation with the cationic surfactants at concentrations well below the critical micelle concentration, while this is inhibited with the anionic SDS, as demonstrated from conductivity measurements. The interaction with cationic surfactants only shows a small dependence on alkyl chain length or counterion and is suggested to be dominated by electrostatic interactions. In contrast to previous studies with the nonionic C₁₂E₅, both the cationic and the anionic surfactants quench the PBS-PFP emission intensity, leading also to a decrease in the polymer emission lifetime. However, the interaction with these cationic surfactants leads to the appearance of a new emission band (~525 nm), which may be due to energy hopping to defect sites due to the increase of PBS-PFP interchain interaction favored by charge neutralization of the anionic polymer by cationic surfactant and by hydrophobic interactions involving the surfactant alkyl chains, since the same green band is not observed by adding either tetramethylammonium hydroxide or chloride. This effect suggests that the cationic surfactants are changing the nature of PBS-PFP aggregates. The nature of the polymer and surfactant interactions can, thus, be used to control the spectroscopic and conductivity properties of the polymer, which may have implications in its applications.

Introduction

Conjugated polymers (CPs) are organic semiconductors¹ and are currently the focus of great interest in the scientific community due to their applications in a wide variety of fields. Since the first observation of light emission from CPs,² research on these systems has led to their rapid development for use in areas such as multicolor organic electroluminescent displays, lasers, and solar cells.³ Particular practical importance has been placed on the development of ink jet patterning methods for preparation of light-emitting polymer-based multicolor displays as a consequence of their low cost, rapid production, and high resolution.⁴ Optical properties of CPs such as fluorescence efficiency or Förster resonance energy transfer, or other physical properties, such as electrical conductivity, are markedly affected by the presence of various small molecules, such that CPs can provide a collective response.⁵ As a consequence, CPs show considerable potential as chemical and biological sensors.^{6,7}

Within the great variety of conjugated polymers which have been studied, the two families which have dominated the area for luminescent systems are the poly(*p*-phenylenevinylenes), which were the first reported systems for light emitting diodes,^{2,1} and *p*-phenylene based polymers, such as polyfluorene (PF). Other well-established CPs include functionalized polydiacetylenes, polysilanes, polythiophenes, and poly(alkylbithiazoles).^{8,9}

For CPs, it is desirable to get the maximum π -conjugation along the main chain with substituents that guarantee the solution processing of the materials without distorting the aromatic building blocks. These aims are favorably reached with polymers containing 9,9-substituted fluorene moieties.¹⁰ In addition, PF based polymers have excellent optical and electronic properties; they can be synthesized with high purity, generally show good chemical and photochemical stability, emit in the blue part of the visible spectrum, and are durable under operation in light-emitting diodes.^{11,12,13} Moreover, polyfluorenes can show regular supramolecular packing and form liquid crystalline structures.¹⁰

Optical properties of polyfluorenes can be modified by varying the polymer structure (*synthesis via*).^{10,14} Some of the synthetic strategies which have been followed to improve their applications include extended conjugation by using more planar

* To whom correspondence should be addressed. Phone: (H.D.B.) +351+239+854482. Fax: (H.D.B.) +351+239+827703. E-mails: (H.D.B.) burrows@ci.uc.pt; (M.J.T.) mjtapia@ubu.es.

[†] Universidad de Burgos.

[‡] Universidade de Coimbra.

[§] Bergische Universität Wuppertal.

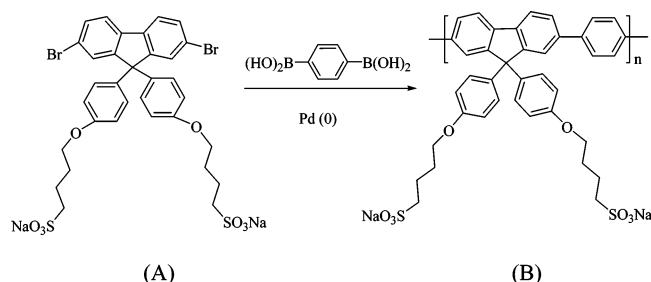


Figure 1. Synthesis and structure of poly{[1,4-phenylene-[9,9-bis(4-phenoxybutylsulfonate)]fluorene-2,7-diyl} copolymer.

indeno[1,2-b]fluorene units, suppression of long wavelength emitting aggregates by attachment of bulky dendron groups or tuning the emission color across the visible spectrum by incorporating perylene dye units on the main chain.¹⁴ Interest has recently focused on synthesis of water soluble ionic conjugated polymers, and with these conjugated polyelectrolytes, their optical and chemical properties can be also tuned by combining them with the appropriate surfactants,¹⁵ since the polymer–surfactant complexes may have very different conformations from that of the free polymer.¹⁶

It has been proposed that this change of optical properties of water soluble conjugated materials upon addition of surfactants be called “surfactochromicity”.¹⁷ The effects produced by the conjugated polyelectrolyte–surfactant interaction are highly dependent on the system. Complexation between the anionic polymer poly(2,5-methoxypropyloxysulfonatephenylenevinylene) (MPS-PPV) and the cationic surfactant dodecyltrimethylammonium bromide enhances the fluorescence quantum yield dramatically, which is noticeable even at a surfactant:polymer ratio as low as 1:100 (surfactant molecules per repeat unit of the polymer).¹⁵ These marked changes are attributed to a conformational change of the polymer, suggesting that the surfactant chains are oriented along the polymer backbone to maximize their interactions.¹⁵ However, the surfactochromicity is not only observed as a consequence of the interaction between conjugated polyelectrolytes and oppositely charged surfactants but has also been seen with uncharged water soluble sugar-substituted poly(*p*-phenyleneethynylene)–nonionic surfactant systems.¹⁷ In this case a blue-shifted emission and a break up of aggregates are observed for surfactant concentrations that are well above the surfactant critical micelle concentration.¹⁷

We have recently reported marked changes in the optical properties and molar conductivity of the anionic poly{[1,4-phenylene-[9,9-bis(4-phenoxy-butylsulfonate)]fluorene-2,7-diyl} copolymer (PBS-PFP, Figure 1B) in aqueous solutions in the presence of the nonionic surfactant *n*-dodecyl pentakis-(ethylene glycol) ether (C₁₂E₅).¹⁸ The main changes observed are as follows: a large increase in the fluorescence quantum yield and lifetime, a blue shift in the maximum emission spectra, and an increase in the molar conductivity. All these changes are clearly observed above the C₁₂E₅ critical micelle concentration and are attributed mainly to the breaking up of PBS-PFP aggregates and the incorporation of isolated chains of PBS-PFP in micelles.

In this paper we extend this work to a study of the interaction of PBS-PFP with ionic surfactants using electronic absorption and emission spectroscopy and electrical conductivity. Cationic alkyltrimethylammonium halides of varying chain length or counterion and the anionic sodium dodecyl sulfate have been studied. As will be shown, the behavior with the ionic surfactants is very different from that observed with the nonionic surfactant (C₁₂E₅).

Experimental Section

Reagents. Polyfluorene Synthesis. The water soluble PPS-PFP (Figure 1B) was synthesized through the following procedure:

2,7-Dibromo-9,9-bis(4-sulfonylbutoxyphenyl)fluorene (Dibromo Monomer). The dibromo monomer, 2,7-dibromo-9,9-bis(4-sulfonylbutoxyphenyl)fluorene (Figure 1A) was synthesized in three steps. The first involves oxidation of 2,7-dibromofluorene with sodium dichromate/acetic acid to give 2,7-dibromofluorene-9-one. In the second step, 2,7-dibromofluorene-9-one was reacted with phenol/methane sulfonic acid to give 2,7-dibromo-9,9-bis(4-hydroxyphenyl)fluorene. The final reaction involved the etherification of 2,7-dibromo-9,9-bis(4-hydroxyphenyl)fluorene with 1,4-butane sultone to 2,7-dibromo-9,9-bis(4-sulfonylbutoxyphenyl)fluorene in dioxane/NaOH. The monomer was obtained in 71% yield (for the three steps).

Poly[9,9-bis(4-sulfonylbutoxyphenyl)fluorene-co-1,4-phenylene] (PBS-PFP, Suzuki-Type Coupling). For the preparation of the copolymer, a mixture of 2,7-dibromo-9,9-bis(4-sulfonylbutoxyphenyl)fluorene (0.824 g, 1 mmol), 1,4-phenylenediboric acid (0.166 g, 1 mmol), Pd(PPh₃)₄ (50 mg), Na₂CO₃ (1.0 g) in 5 mL of distilled water, 50 mL of toluene, and 5 mL of butanol was reacted for 3 days at 135 °C (reflux). The aqueous layer was washed with chloroform and concentrated to dryness. The residue was redissolved in water and purified by dialysis using a membrane with a cutoff of 3500 to yield 0.50 g (54%) of poly[9,9-bis(4-sulfonylbutoxyphenyl)fluorene-co-1,4-phenylene] as a slightly brown powder.

The number average molecular weight of the polymer determined by using GPC(NMP/LiBr) is $M_n = \sim 6500$. Taking the monomer unit molecular weight as 740.8, this indicates an average of about 9 monomers/chain. The polymer was characterized by its ¹H NMR spectrum (300 MHz, D₂O; ppm): δ 6.8–7.9 (ar-H), 3.4–4.0 (α, δ -CH₂), 1.2–2.0 (β, γ -CH₂).

Reagents and Solution Preparation. The cationic surfactants, cetyltrimethylammonium bromide (CTAB, CH₃(CH₂)₁₅N(CH₃)₃Br), tetradecyltrimethylammonium bromide (TTAB, CH₃(CH₂)₁₃N(CH₃)₃Br), dodecyltrimethylammonium bromide (DoTAB, CH₃(CH₂)₁₁N(CH₃)₃Br), dodecyltrimethylammonium chloride (DoTAC, CH₃(CH₂)₁₁N(CH₃)₃Cl), didodecyltrimethylammonium bromide (DDAB, (CH₃(CH₂)₁₁)₂N(CH₃)₂Br), decyltrimethylammonium bromide (DeTAB, CH₃(CH₂)₉N(CH₃)₃Br), the anionic surfactant: sodium dodecyl sulfate (SDS, CH₃(CH₂)₁₁OSO₃Na), tetramethylammonium hydroxide pentahydrate, and hydrochloric acid were purchased from Sigma-Aldrich and used without further treatment. Solutions were prepared using Millipore-Q water with a PBS-PFP concentration around 6×10^{-3} g/L and were kept under continuous stirring overnight before being used for the spectroscopic or conductivity measurements.

Apparatus and Methods. Spectroscopic Measurements. Absorption spectral measurements were made in 1 cm quartz cuvettes on a Shimadzu UV-2100 spectrophotometer. The steady-state fluorescence spectra were measured with the Fluorolog 3-22 instrument with a 2.5 nm excitation bandwidth and 1.25 nm emission bandwidth. Fluorescence decays were measured using a home-built time-correlated single-photon counting apparatus consisting of an IBH NanoLED ($\lambda_{exc} = 373$ nm) as excitation source, Jobin-Ivon monochromator, Philips XP2020Q photomultiplier, and Canberra instruments Time-to-amplitude converter and multichannel analyzer. Alternate measurements (1000 counts/cycle), controlled by Decay software (Biodinâmica-Portugal), of the pulse profile at 373 nm and the sample emission were performed until $(1-2) \times 10^4$ counts at

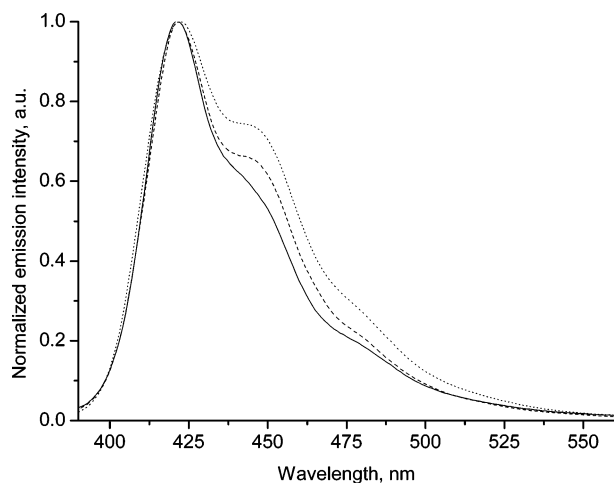


Figure 2. Normalized emission spectra of PBS-PFP in aqueous solution for various polymer concentrations: 6.4×10^{-4} , 2.6×10^{-3} , and 5.1×10^{-3} g/L, solid, dashed, and dotted lines, respectively.

the maximum were reached.¹⁹ The fluorescence decays were analyzed using the modulating functions method of Striker with automatic correction for the photomultiplier “wavelength shift”.²⁰ Although the lifetimes measured are at the limits of the time resolution of our system, reproducible trends of the surfactant on the decays were observed. All experiments were carried out at room temperature (293 K).

Conductivity Measurements. Solution electrical resistances were measured with a Wayne-Kerr model 4265 automatic LCR meter at 1 kHz. A Shedlovsky-type conductance cell was used.²¹ The cell constant (approximately 0.8465 cm^{-1}) was determined to $\pm 0.02\%$ from measurements with KCl (reagent grade; recrystallized and dried using the procedure and data from Barthel *et al.*²²). Measurements were made at 25.00 ± 0.01 °C in a Grant thermostat bath.

Results and Discussion

1. PF Concentration Effect. In relatively concentrated aqueous samples (absorbance at 381 nm around 0.3) of PBS-PFP, precipitation of the sample is observed with time, leading to decreases in both absorbance and fluorescence intensities. This is probably due to aggregation of the polymer, as has been widely described for polyfluorenes.^{10,18,23} However, this decrease in PBS-PFP absorbance and emission intensities is negligible if freshly prepared dilute stock solutions ($\approx 6 \times 10^{-3}$ g/L; absorbance at 381 nm around 0.1) are kept stirred until the moment of being used (at least overnight).

To study the effect of polymer concentration, the absorption and emission spectra and the molar conductivity of aqueous samples have been followed at various concentrations.

Absorption and Emission Spectra. The PBS-PFP absorption spectrum in aqueous solution shows a maximum around 381 nm. For freshly prepared aqueous solutions, the absorbance at this maximum follows the Beer–Lambert law over the concentration range 6.4×10^{-4} to 5.1×10^{-3} g/L (ca. 9.8×10^{-8} to 7.9×10^{-7} M in terms of polymer molecular weight). This means that although there may be significant interactions between the polymer chains, as shown by small-angle neutron scattering (SANS) measurements,²⁴ over this range of polymer concentrations PBS-PFP can be considered as functioning as a single unit.

The fluorescence spectrum of PPS-PFP (Figure 2) displays two maxima around 424 and 448 nm and a shoulder at 475 nm. The intensity of the main emission maximum (424 nm)

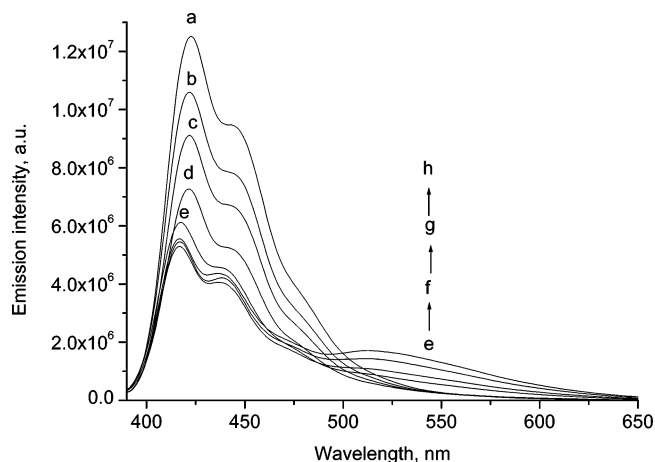


Figure 3. Emission spectra of PBS-PFP in aqueous solution (6.4×10^{-3} g/L, 8.6×10^{-6} monomer molar concentration) (a) and with CTAB additions: 3.3×10^{-7} M (b), 3.7×10^{-7} M (c), 4.6×10^{-7} M (d), 3.9×10^{-6} M (e), 7.8×10^{-6} M (f), 1.6×10^{-5} M (g), 3.9×10^{-5} M (h) (excitation wavelength, 381 nm).

increases approximately linearly with the polymer concentration (9.8×10^{-8} to 7.9×10^{-7} M in terms of polymer). Increases of the emission at 448 and 475 nm are also observed with PBS-PFP concentration. However, upon normalization of the emission intensity at this maximum, the effect is more pronounced at 448 nm, which indicates that concentration affects the vibronic structure, possibly as a result of changes in aggregate structure.

Conductivity. Since PBS-PFP is a polyelectrolyte, the effect of its concentration on the electrical conductivity has also been studied in aqueous solutions and the molar conductivity (Λ) calculated from this using

$$\Lambda = (\kappa - \kappa_0)/(c \times 1000) \quad (1)$$

[κ and κ_0 are specific conductances of solution, c is the polymer concentration ($(1.58\text{--}1.49) \times 10^{-6}$ M)]. The experimental specific conductance is around $3.5 \times 10^{-5} \text{ S m}^{-1}$, and the molar conductivity depends on the square root of the concentration, in agreement with the Kohlrausch equation¹³

$$\Lambda = \Lambda^0 - Ac^{1/2} \quad (2)$$

($\Lambda^0 = 0.36 \pm 0.01 \text{ S m}^2 \text{ mol}^{-1}$; $A = 8.50 \pm 0.27 \text{ S mol}^{-3/2} \text{ m}^{7/2}$.) The molar limiting conductivity, Λ^0 , is similar to that for other polyelectrolytes in aqueous solution.¹⁴

The fact that the polymer displays Beer–Lambert and Kohlrausch law behavior over the concentration range studied seems to indicate that aqueous PBS-PFP solutions are “well-behaved” and that dilution does not affect the stability of any aggregates present in solution.¹⁸ However, this behavior does not mean that this is a true solution in thermodynamic terms, and, as suggested by SANS, the system is better treated as a very dilute dispersion.

2. Addition of CTAB. The effect of adding CTAB to dilute aqueous solutions of PBS-PFP was studied by UV/visible absorption spectroscopy, fluorescence (steady state and time resolved), and electrical conductivity.

Absorption and Fluorescence Spectra. Upon increasing the CTAB concentration, a decrease in absorbance at the maximum (around 381 nm) was observed. This is consistent with the surfactant interacting with the polymer and changing aggregate structure. In the fluorescence spectrum (Figure 3), CTAB produces a marked quenching of the emission up to surfactant

concentrations of 5×10^{-7} M, followed at higher concentrations by the appearance of a new band around 525 nm. This contrasts dramatically with the fluorescence enhancements seen on adding cationic surfactants to MPS-PPV.¹⁵ In part this may be due to the relatively low molecular weight of the polymer PBS-PFP (approximately 9 repeat units). However, we feel that this is not the only reason, since enhancement of fluorescence of the polymer is seen on adding the nonionic C₁₂E₅.¹⁸ Instead, there may be some intrinsic difference in the behavior of these polymers resulting from the fairly rigid backbone of fluorene copolymers compared with the random coil structure of poly(*p*-phenylenevinylenes). The lack of an isoemissive point in Figure 3 seems to indicate that the appearance of this long emission band (525 nm) does not result from any simple two-state equilibrium with the polymer but is rather induced by more complex external interactions, such as chain aggregation, promoted by the CTAB surfactant. The green band at 525 nm starts to be clearly observed for CTAB concentrations around 4×10^{-6} M (spectrum e). All these concentrations are well below the surfactant critical micelle concentration (cmc, 8×10^{-4} M at 25 °C²⁵). As both the quenching and the observation of the new emission band at 525 nm are observed at CTAB concentrations well below the cmc, they are probably not due to micellization, but are associated with specific interactions between the polymer and the oppositely charged surfactant. The concentration at which this occurs is frequently referred to as a critical association concentration (cac).²⁶ In addition, the main PBS-PFP emission maximum is blue-shifted (from 424 to 418 nm) upon increasing the CTAB concentration above 7.8×10^{-6} M, Figure 3.

We will defer discussion of the quenching until later. Several explanations have been proposed for the appearance of the green emission band (525 nm) in polyfluorenes, including reordering of polymer chains, leading to aggregate²⁷ or excimer formation,^{28,29} and emission from ketonic defects incorporated into the polymer backbone in the form of 9-fluorenones. Recently, Romaner *et al.* have provided experimental evidence against excimer or aggregate formation as being the primary source for the low-energy emission band in polyfluorene-type materials and have supported the explanations that keto defect sites are responsible for this fluorescence.²⁹ These defects have been identified in all methylene-bridged poly(*p*-phenylene)-type materials upon thermal, photochemical, and/or electrical degradation^{10,29,30} and have been attributed to oxidative processes, leading to 9-fluorenone generation, with the effect being more important for polymers with hydrogen at the bridge position (9-position) and less significant in poly(9,9-dialkylfluorenes).³⁰ However, in the present study, it is not clear why any oxidative process can be induced by surfactant addition to PBS-PFP (9,9-dialkylfluorene-alternating phenylene copolymer). Although such defects can be already generated during the polymer synthesis,²⁹ with the relatively low molecular weight polymer used, not many fluorenone defects are expected to be present in single chains of PPS-PFP. Further, although they may be generated during photooxidation, no green band (525 nm) was detected in a photodegradation study of the polymer that will be reported elsewhere.

However, despite the controversy around the origin of the green band in the emission spectra of polyfluorene-type polymers and regardless of the explanation considered, a common point in which all the theories on this effect converge is the fact that interchain interactions favor this green emission by excitation energy transfer to lower energy emission sites. This is obvious both for the aggregate and excimer proposals.

Although it is less evident with the 9-fluorenone emission (keto defects) proposal, quantum chemical calculation and related experiments have revealed that the intrachain migration rate in conjugated polymers is almost 2 orders of magnitude lower than the interchain migration, such that energy hopping between chains is favorable.³¹ This is the reason the 9-fluorenone emission is predominantly observed in the solid state at rather high 9-fluorenone concentrations and strongly diminishes in isolated molecules in solution or in solid polymers with increased interchain distances (bulky side groups, blends with other inert polymers as polystyrene). For isolated polymer chains in solution it was found that an average of at least 1.5% 9-fluorenone moieties need to be incorporated into the PF backbone to observe the low-energy emission.³² It has recently been stated by Sims *et al.* that fluorenone formation is a *necessary but not sufficient* condition for the appearance of the green band. The fluorenone moieties are efficient quenchers of intrachain emission but additional interchain (or intersegment) interactions may be required for the appearance of the green band.³³

To probe whether the increase in the 525 nm band produced on adding CTAB is due to the increase of interchain interactions or polymer agglomeration, some fluorescence excitation and turbidity experiments were made both by changing the surfactant concentration and by maintaining CTAB concentration constant and diluting the PBS-PFP solution. The scattering at the excitation wavelength increases on increasing CTAB concentration, Figure 4 A, and on increasing the PBS-PFP solution for a constant surfactant concentration, Figure 4B. The scattering increase with the polymer concentration can be attributed to changes in the polymer aggregation. Similarly, CTAB addition can be assumed to induce ordering of polymer aggregates as a result of neutralization of the anionic charge of the polymer by the cationic surfactant, since the changes induced in the scattering (Figure 4B) are very similar to those observed on increasing the polymer concentration (Figure 4A).

To obtain further information on the nature of the green emission, the excitation spectra of the samples were recorded at two emission maxima (422 and 525 nm) with several CTAB concentrations, Figure 4C. The normalized excitation spectra (CTAB, 3.9×10^{-5} M) are slightly different for the two bands, which indicate they correspond to somewhat different kinds of PBS-PFP chain segments. Significant differences are observed for the wavelength region below 360 nm. This region with somewhat increased excitation energy represents copolymer chains with somewhat increased structural disorder within the so-called "density of states". The increased disorder may be coupled to the surfactant-induced aggregation into "solid" polyelectrolyte-surfactant complexes. The aggregation of polyfluorenes is often accompanied by a considerable spectral broadening of the long-wavelength absorption band, and, possibly related to this, the excitation spectrum for the 525 nm emission band in PBS-PFP changes with increasing CTAB concentration and, consequently, with ongoing aggregation.

Very similar changes in the excitation spectra are observed not only for increasing CTAB concentration (Figure 4C) but also for increasing PBS-PFP concentration (Figure 4D), which also supports the idea that surfactant addition causes an increase of the polymer interchain interactions.

Assuming electrostatic interactions are dominant, the negatively charged SO₃⁻ groups of PPS-PFP are likely to interact with the positive headgroups of the surfactant-inducing aggregation into neutral polyelectrolyte-surfactant complexes over a CTAB concentration range which corresponds to the theoretic-

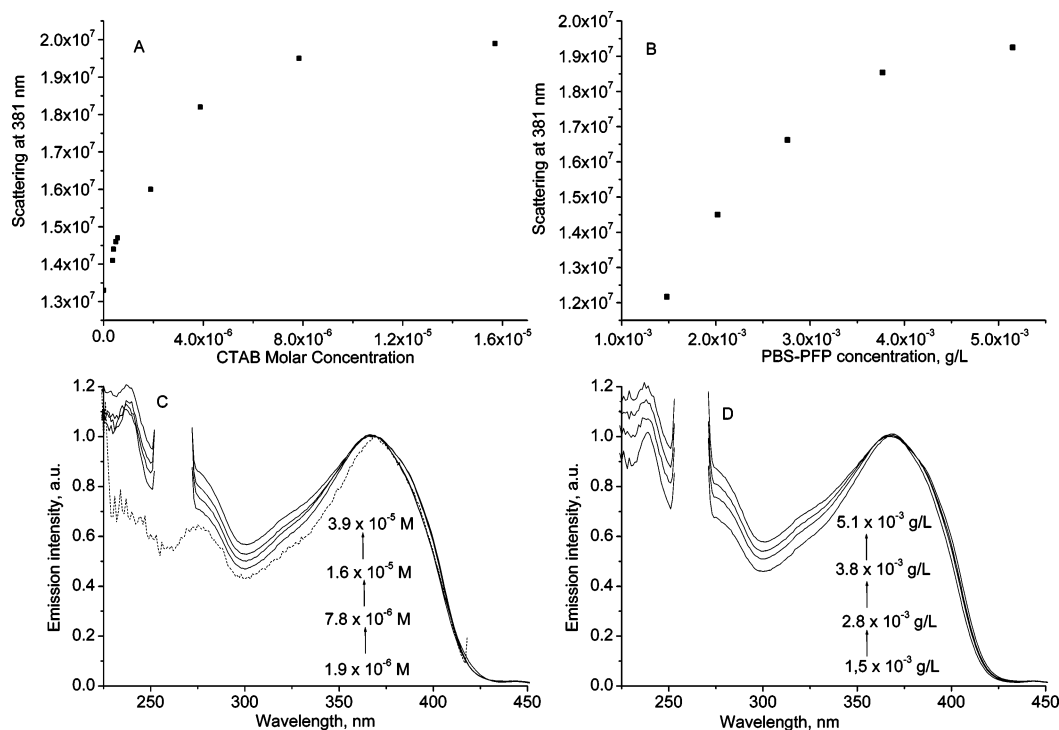


Figure 4. (A) Scattering at 381 nm versus CTAB concentration (PBS-PFP, 6.4×10^{-3} g/L), (B) scattering at 381 nm versus PBS-PFP concentration (CTAB, 2.0×10^{-4} M), (C) continuous lines) normalized excitation spectra for 6.4×10^{-3} g/L PBS-PFP (emission wavelength, 525 nm) for several CTAB concentrations and (dashed line) normalized excitation spectrum (emission wavelength, 422 nm; CTAB, 3.9×10^{-5} M; slits, 1.25: 2.50 nm), and (D) normalized excitation spectra for 2.0×10^{-4} M CTAB (emission wavelength, 525 nm) for several PBS-PFP concentrations. A band at 261 nm (half of the emission wavelength) is an artifact and has been removed.

cal value for neutralization of the negative charges of the polymer solution (1.6×10^{-5} M). This is expected to lead to an increased rate of excitation energy transfer in the solid (aggregated) state, allowing the emission band at 525 nm to be clearly observed; see Figure 3. As a further consequence of the formation of PBS-PFP/CTAB aggregates, the polarity of the polymer environment decreases, which could explain the blue shift of the main emission band at 424 nm, Figure 3.

However, the green band is not observed when PBS-PFP interacts with other positively charged single-chain or gemini-type arginine-based surfactants with a more bulky, branched structure.³⁴ We feel that the branched structure of these surfactants reduces the ability for interchain interactions between the conjugated backbones and suppresses the formation of "solid" polyelectrolyte-surfactant complexes, which seems to be the key prerequisite for observation of the emission feature at 525 nm. Further, the interaction of PBS-PFP with the nonionic surfactant C₁₂E₅ also does not lead to the observation of the green emission band since this surfactant cannot induce polymer aggregation by charge compensation but, instead, tends to break up PBS-PFP aggregates in aqueous solution.¹⁸

Lifetime. Time-resolved fluorescence experiments were carried out by adding various concentrations of CTAB (3.2×10^{-7} to 2.0×10^{-4} M) to an aqueous PBS-PFP solution (6×10^{-3} g/L), exciting close to the absorption maximum (373 nm), recording the emission at 420 nm and for the highest CTAB concentrations studied (3×10^{-5} and 2×10^{-4} M) also at 530 nm. The emission decay at 420 nm (at all CTAB concentrations) and at 530 nm (for low surfactant concentrations) can be fitted to a single exponential. The experimental results for the decrease in this lifetime with increasing CTAB concentration are shown in Figure 5, which demonstrates a more marked quenching at CTAB concentrations ($\leq 10^{-6}$ M) well below the surfactant cmc. For the decay at 530 nm, an additional component with a

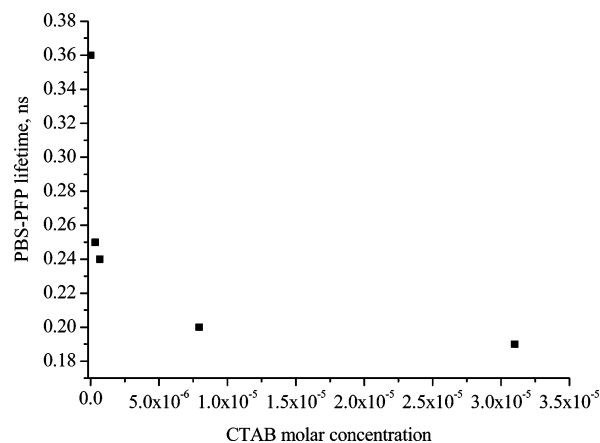


Figure 5. PBS-PFP fluorescence lifetime versus CTAB concentration.

lifetime of 1.5–1.7 ns, but with a very small contribution (<5%), was needed at the highest surfactant concentrations to properly fit the decays. Full details are given elsewhere.³⁵

Assuming the model of the electrostatic interaction between PBS-PFP and CTAB and taking into account results of both steady-state and time-resolved studies, it can be seen that the polymer-surfactant interaction has both static and dynamic components. Detailed explanation for these observations requires information on the aggregate species present. However, qualitatively, the long lifetime is close to that of molecular fluorenone in solution (3.0 ns)³³ and of the same order of magnitude as those of the green band in photooxidized poly(9,9-dioctylfluorene), 6.0 ns.³³ The small contribution of the long-lifetime component suggests that the fluorenone defects, if present, are in very small proportion. Further insight into the nature of the CTAB-PBS-PFP interactions is gained by electrical conductivity measurements.

Conductivity. Electrical conductivity of surfactant solutions

TABLE 1: Changes in the Conductivity of PBS-PFP and Surfactant Aqueous Solutions

| | $\Delta c/(10^{-3} \text{ M})$ | $\kappa = A + Bc$ | | | |
|----------------|--|---|--------------------------------------|-------|----------------------------------|
| | | $A/(\mu\text{S cm}^{-1})$ | $B/(\text{mS cm}^{-1}\text{M}^{-1})$ | R^2 | $\text{cac}/(10^{-3} \text{ M})$ |
| CTAB | 0.2–0.9 (pre m) | 0 | 94.4 (0.1) | 0.999 | 0.964 ³⁶ |
| | 1.0–3.4 (post m) | 69.3 (0.4) | 22.5 (0.01) | 0.999 | (0.005) |
| PBS-PFP + CTAB | 3.0×10^{-4} to 7.1×10^{-3} (pre-m) | 1.6 (0.01) | 157.4 (4.4) | 0.998 | 0.013 |
| | 1.0×10^{-2} to 0.2 (post-m) | 2.7 (0.3) | 72.2 (2.4) | 0.998 | (0.003) |
| PBS-PFP + SDS | 3×10^{-4} to 3.2×10^{-2} | 1.1 (0.1) | 70.4 (0.7) | — | |
| | 3.2×10^{-2} to 5.0×10^{-2} | 1.0 (0.0) | 75.4 (1.2) | 0.999 | |
| | 5.0×10^{-2} to 0.20 | positive deviation from a straight line | | | |

provides an excellent method for characterizing micelles or other aggregate species present. The conductivity of a surfactant solution increases linearly with concentration, but the slopes and intercepts of the lines are different before (pre-m, Table 1) and after (post-m) micelle formation. The cmc is taken as the concentration at which the lines cross, and for CTAB in aqueous solution, the value $9.6 \times 10^{-4} \text{ M}$ ³⁶ has been determined (Table 1).

The same procedure has been followed by adding CTAB to aqueous PBS-PFP solutions with a polymer concentration around $6.4 \times 10^{-3} \text{ g/L}$ ($8.6 \times 10^{-6} \text{ mol}$ (of repeat unit)/L). However, although in the presence and absence of PBS-PFP, the specific conductance, κ , increases linearly with the surfactant concentration, and the data can be fitted to two straight lines, indicating critical aggregation phenomena, the crossing points of the plots in the presence and absence of PBS-PFP are very different. The value in the presence of PBS-PFP, taken as the critical association concentration (cac), is $1.3 \times 10^{-5} \text{ M}$ under these conditions (see Table 1). This is nearly 2 orders of magnitude lower than the cmc. The free energy per mole surfactant, G_{PS}^0 , for the reaction free micelle/polymer-bound micelle, given by²⁶

$$G_{\text{PS}}^0 = RT \ln(\text{cac}/\text{cmc}) \quad (3)$$

where R is the universal gas constant and T the temperature is a convenient measure of the strength of the interaction between the surfactant and the polymer. In CTAB/PBS-PFP $G_{\text{PS}}^0 = -10.6 \text{ kJ mol}^{-1}$. Apparently, the PBS-PFP surface is inducing nucleation thus favoring CTAB aggregation with it through electrostatic interactions. At the cac, the surfactant:polymer molar concentration ratio (expressed in terms of PBS-PFP repeat units) is approximately 1.6:1, which is close to the electroneutrality ratio of 2:1, since every monomer unit has two anionic chains.

If the interaction between CTAB and PBS-PFP is mainly electrostatic, it is anticipated that the addition of a negatively charged surfactant, such as sodium dodecyl sulfate (SDS), will lead to markedly different effects on the spectroscopic and electrical conductivity behavior.

3. SDS Addition. The effect of addition of SDS (3.3×10^{-8} to $1.6 \times 10^{-4} \text{ M}$) to an aqueous solution of PBS-PFP ($6.0 \times 10^{-3} \text{ g/L}$) was studied through the spectroscopic and conductivity properties.

No significant changes in the absorption spectrum were observed on adding SDS to aqueous solutions of PBS-PFP, although there was a slight increase in the background scattering. At higher surfactant concentrations, phase separation occurred. In the fluorescence spectrum, quenching of the PBS-PFP emission was seen on adding SDS, although there was no effect on the PBS-PFP fluorescence lifetime (within the time resolution of our system $\geq 150 \text{ ps}$). In contrast to the behavior with the cationic surfactant, no new emission band was observed at 525 nm, which supports the previous argument that this band with

CTAB is a consequence of the electrostatic interaction between the positively charged surfactant and the negative groups of PBS-PFP. The lack of effect of SDS on the polymer emission lifetime suggests that electrostatic repulsion is minimizing aggregation and that in this case the polymer is not working as a nucleation nucleus. This is supported by electrical conductivity measurements (Table 1). With the anionic surfactant, SDS, the behavior is different from that observed for CTAB. All electrolytic conductivity data can only be fitted to a single straight line, with no evidence for the formation of any aggregate in the SDS concentration range studied (3.0×10^{-7} to $5.0 \times 10^{-5} \text{ M}$).

4. Other Cationic Surfactants. As the association between the cationic surfactant (CTAB) and PBS-PFP seems to be driven by electrostatic interactions, the behavior of a range of other cationic surfactants with PBS-PFP has been studied as a function of alkyl chain length ($\text{CH}_3(\text{CH}_2)_n\text{N}(\text{CH}_3)_3\text{Br}$, $n = 9$ (DeTAB), 11 (DoTAB), 13 (TTAB), Figure 6A1,A2, and counterion (dodecyltrimethylammonium chloride and bromide, DoTAC, DoTAB) and of having a double alkyl chain didodecyltrimethylammonium bromide (DDAB, $(\text{CH}_3(\text{CH}_2)_{11})_2\text{N}(\text{CH}_3)_2\text{Br}$), Figure 6B1,B2.

Qualitatively, the effects of adding surfactant on the emission spectra for all these systems show behavior similar to that presented for CTAB in Figure 3, with quenching of the main fluorescence band at around 422 nm and the appearance of a new emission band at around 525 nm. The evolution of these two main bands versus the surfactant concentrations is shown for all these surfactants in Figure 6.

In Figure 6A1 and 6B1 the ratio between the emission intensity of the main emission band (422 nm) in the presence and absence of surfactant is plotted versus the surfactant concentration. As with CTAB, the first surfactant additions provoke a pronounced emission quenching, while for the highest surfactant concentration a plateau is reached. Only in the case of the double chain surfactant DDAB does the emission intensity recover slightly for intermediate and high surfactant concentrations (2.2×10^{-5} to $1.6 \times 10^{-4} \text{ M}$).

Considering the effect of the counterion, comparison of the behavior of PBS-PFP with DoTAB and DoTAC, which have the same surfactant chain but different counterions (bromide and chloride), it is possible to obtain some insight into the mechanism of quenching of the fluorescence at 422 nm. Halide ions are known to quench fluorescence of aromatic hydrocarbons,³⁷ and the stronger quenching of the main emission band at 422 nm in DoTAB than in DoTAC (Figure 6B1) suggests counterion quenching must play some role in this. This may be due to a heavy atom effect³⁸ although other mechanisms are also possible.³⁷ This cannot be the only mechanism, since it does not explain either the differences in behavior of single-chain and double-chain surfactants in Figure 6B1 or the effects of chain length in Figure 6A1. It seems probable that much of the quenching comes from increased interactions between conjugated polymer chains resulting from ordering of the

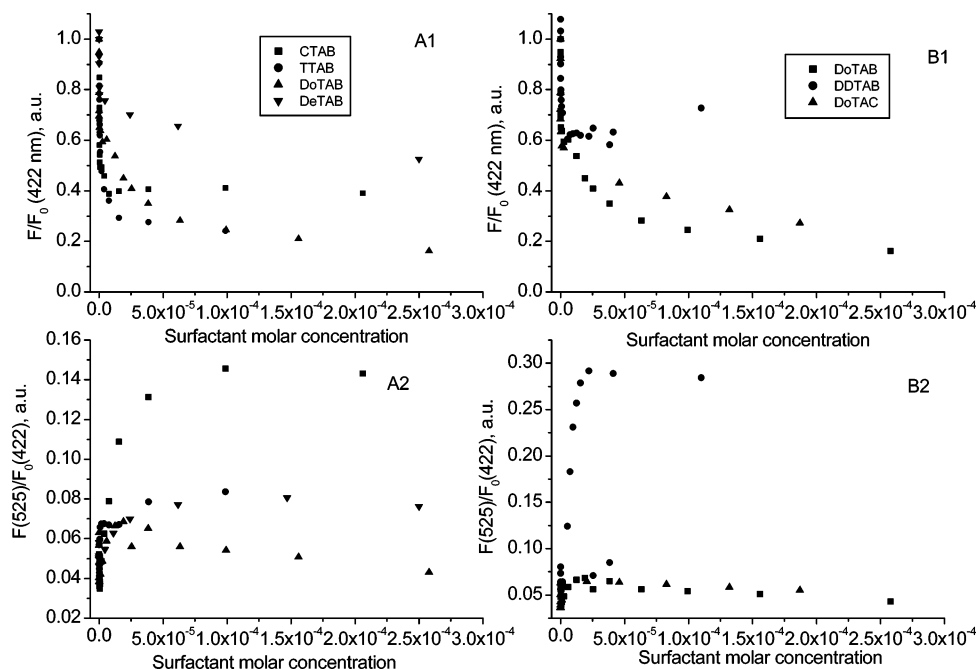


Figure 6. Normalized emission intensity at 422 (A1) and 525 nm (A2) as a function of the surfactant molar concentration for various cationic surfactants. Chain length effects are shown in A1 and A2, while the effects of counterion and double alkyl are given in B1 and B2.

aggregates induced by the surfactant chains. A similar effect may be responsible for the quenching induced by SDS.

In Figure 6A2 and 6B2 the ratio between the fluorescence intensity at 525 nm to that at 422 nm in the absence of surfactant (thus allowing correction for the small differences in the initial surfactant concentration) is plotted versus the surfactant concentration. In this case, the emission intensity of the band at 525 nm increases and a plateau is reached for the highest surfactant concentrations. The plateau is normally reached for a concentration ratio between the polymer repeat unit and the surfactant molar concentration close to 0.5 (1 polymer repeat unit to 2 surfactant molecules), indicating neutralization of all the polymer charged groups. This is very similar to the surfactant:repeat unit concentration ratio (1.6:1) seen in the electrical conductivity results with CTAB (see above) and indicates that surfactant aggregation involves neutralization of the PBS-PFP anionic charge by electrostatic interaction with the cationic surfactant, which occurs well below the cmc. The observations that the surfactant aggregation does not depend on surfactant chain length seems to support the idea that the dominant effect is charge neutralization, and contrast with other polymer/surfactant systems, where hydrophobic interactions play a major role on the association phenomena.²⁶

To check the role of surfactancy in these experiments, tetramethylammonium ions were added to PBS-PFP aqueous solution in the same concentration range used for the surfactants using both the hydroxide at its natural pH and the chloride obtained by neutralization of this base with HCl. Similar results were observed with hydroxide and chloride, with the PBS-PFP emission being quenched up to a polymer repeat unit:tetramethylammonium ratio close to 1:1. However, in contrast to the experiments with the tetraalkylammonium surfactants, no green band emission at 525 nm was observed. This means that the hydrophobic interactions between the surfactant molecules and/or the surfactant molecules and polymer chains play a major role in producing the green band at 525 nm in these systems, probably as a consequence of increased interchain interaction between the conjugated backbones.

This is corroborated by the effect of the nature of the surfactant alkyl chain on the formation of the 525 nm band, since it is most effectively induced by the most hydrophobic surfactants, with the double alkyl chain surfactant, DDAB (Figure 6B2), being most effective, followed by the surfactant with the longest alkyl chain, CTAB (Figure 6A2). The presence of bromide or chloride as counterion does not seem to affect the emission maximum at around 525 nm (Figure 6B2), indicating that these only effect the initial quenching of the 422 nm band and do not significantly affect aggregation.

Conclusion

The interaction between the conjugated polymer PBS-PFP, a negatively charged polyelectrolyte, and cationic and anionic surfactants has been studied by combining absorption and fluorescence spectroscopy and electrical conductivity measurements.

The interaction between this polymer and the surfactants appears to be mainly governed by electrostatic interactions between the charged groups in such a way that aggregation with cationic surfactants is favored for a ratio of monomer to surfactant molar concentration close to electroneutrality (1:2), whereas that with the anionic surfactant SDS is inhibited, as it is shown from the conductivity measurements.

Both cationic and anionic surfactants quench the emission intensity of PBS-PFP, and in the cases of the cationic surfactants, a new band at low energies (~ 525 nm) is observed. The new band is assumed to be caused by the polymer agglomeration as a consequence of the interaction with the cationic surfactants, and it is clearly observed after polymer charge neutralization. The copolymer aggregation favors the interchain excitation energy transfer to defect sites and speeds up the PL decay, resulting in an exponential decrease of the fluorescence lifetime. With the anionic surfactant SDS, the electrostatic repulsion between the surfactant and the negatively charged polymer prevents this association, and no change is observed in the PBS-PFP lifetime. Formation of the 525 nm emission band is, however, favored by double chain (DDAB) or longer alkyl chain

(CTAB) cationic surfactants due to hydrophobic interactions. A small heavy atom effect is also observed by comparing the data of two cationic surfactants with chloride or bromide counterions.

In a previous study on the behavior of PBS-PFP in the presence of the nonionic surfactant *n*-dodecyl pentakis(ethylene glycol) ether (C₁₂E₅),¹⁸ the importance of hydrophobic interactions between surfactant and polymer on the photophysical behavior in aqueous solutions was indicated. The present study shows that electrostatic forces may also be important. The nature of the polymer and surfactant interactions can, thus, be used to control the spectroscopic and conductivity properties of the polymer, which may have implications in its applications.

Acknowledgment. We are grateful for financial support from POCTI/FCT/FEDER, MEC/FEDER (Project MAT2004-03827), MEC/CRUP (Açções Integradas), and BMBF (EKOS collaboration). The Universidad de Burgos is also thanked for support of a short stay by M.J.T. in Coimbra University.

References and Notes

- (1) Hadziioannou, G.; van Hutten, P. F., Eds. *Semiconducting Polymers: Chemistry, Physics and Engineering*; Wiley-VCH: Weinheim, Germany, 2000.
- (2) Burroughes, J. H.; Bradley, A. R.; Brown, A. R.; Marks, R. N.; Mackay, K.; Friend, R. H.; Burns, P. L.; Holmes, A. B. *Nature (London)* **1990**, *347*, 539–541.
- (3) (a) Fan, C.; Plazco, K. W.; Heeger, A. J. *J. Am. Chem. Soc.* **2002**, *124*, 5642–5643. (b) Virgili, T.; Lidzey, D. G.; Bradley, D. D. C. *Synth. Met.* **2000**, *111–112*, 203–206. (c) Bliznyuk, V. N.; Carter, S. A.; Scott, J. C.; Klärner, G.; Miller, R. D.; Miller, D. C. *Macromolecules* **1999**, *32*, 361–369. (d) Palilis, L. C.; Lidzey, D. G.; Redecker, M.; Bradley, D. D. C.; Inbasekaran, M.; Woo, E. P.; Wu, W. W. *Synth. Met.* **2000**, *111–112*, 159–163. (e) Halls, J. J. M.; Arias, A. C.; Mackenzie, J. D.; Wu, W.; Inbasekaran, M.; Woo, E. P.; Friend, R. H. *Adv. Mater.* **2000**, *12*, 498–502.
- (4) Kobayashi, H.; Kanbe, S.; Seki, S.; Kigchi, H.; Kimura, M.; Yudasaka, I.; Miyashita, S.; Shimoda, T.; Towns, C. R. M.; Burroughes, J. H.; Friend, R. H. *Synth. Met.* **2000**, *111–112*, 125–128.
- (5) Liu, B.; Wang, S.; Bazan, G. C.; Mikhailovsky, A. *J. Am. Chem. Soc.* **2003**, *125*, 13306–13307.
- (6) (a) Chen, L.; McBranch, D.; Wang, H.-L.; Helgerson, R.; Wudl, F.; Whitten, D. G. *Proc. Natl. Acad. Sci. U.S.A.* **1999**, *96*, 12287–12292. (b) Chen, L.; Xu, S.; McBranch, D.; Whitten, D. *J. Am. Chem. Soc.* **2000**, *122*, 9302–9303.
- (7) (a) Heeger, O. S.; Heeger, A. J. *Proc. Natl. Acad. Sci. U.S.A.* **1999**, *96*, 12219–12221. (b) Liu, B.; Gaylord, B. S.; Wang, S.; Bazan, G. C. *J. Am. Chem. Soc.* **2003**, *125*, 6705–6714. (c) Lavigne, J. J.; Broughton, D. L.; Wilson, J. N.; Erdogan, B.; Bunz, U. H. F. *Macromolecules* **2003**, *36*, 7409–7412.
- (8) Nanos, J. I.; Kampf, J. W.; Curtis, M. D.; Gonzales, L.; Martin, D. C. *Chem. Mater.* **1995**, *7*, 2232–2234.
- (9) Blondin, P.; Bouchard, J.; Beaupré, S.; Belletête, M.; Durocher, G.; Leclerc, M. *Macromolecules* **2000**, *33*, 5874–5879.
- (10) Scherf, U.; List, E. J. W. *Adv. Mater.* **2002**, *14*, 477–487.
- (11) Charas, A.; Morgado, J.; Martinho, J. M. G.; Alcácer, L.; Lim, S. F.; Friend, R. H.; Cacialli, F. *Polymer* **2003**, *44*, 1843–1850.
- (12) Leclerc, M. *J. Polym. Sci., Part A: Polym. Chem.* **2001**, *39*, 2867–2973.
- (13) Neher, D. *Macromol. Rapid. Commun.* **2001**, *22*, 1365–1385.
- (14) Becker, S.; Ego, C.; Grimsdale, A. C.; List, E. J. W.; Marsitzky, D.; Pogantsch, A.; Setayesh, S.; Leising, G.; Müllen, K. *Synth. Met.* **2002**, *125*, 73–80.
- (15) Chen, L.; Xu, S.; McBranch, D.; Whitten, D. *J. Am. Chem. Soc.* **2000**, *122*, 9302–9303.
- (16) (a) Macknight, W. J.; Ponomarenko, E. A.; Tirrell, D. A. *Acc. Chem. Res.* **1998**, *31*, 781–788. (b) Kabanov, A. V.; Bronich, T. K.; Kabanov, V. A.; Yu, K.; Eisenberg, A. *J. Am. Chem. Soc.* **1998**, *120*, 9941–9942. (c) Kuhn, P. S.; Levin, Y.; Barbosa, M. C. *Chem. Phys. Lett.* **1998**, *298*, 51–56.
- (17) Lavigne, J. J.; Broughton, D. L.; Wilson, J. N.; Erdogan, B.; Bunz, U. H. F. *Macromolecules* **2003**, *36*, 7409–7412.
- (18) Burrows, H. D.; Lobo, V. M. M.; Pina, J.; Ramos, M. L.; Seixas de Melo, J.; Valente, A. J. M.; Tapia, M. J.; Pradhan, S.; Scherf, U. *Macromolecules* **2004**, *37*, 7425–7427.
- (19) Seixas de Melo, J.; Fernandes, P. F. *J. Mol. Struct.* **2001**, *565*, 69–74.
- (20) Striker, G.; Subramaniam, V.; Seidel, C. A. M.; Volkmer, A. *J. Phys. Chem. B* **1999**, *103*, 8612–8617.
- (21) Ribeiro, A. C. F.; Valente, A. J. M.; Lobo, V. M. M.; Azevedo, E. F. G.; Amado, A. M.; Amorim da Costa, A. M.; Ramos, M. L.; Burrows, H. D. *J. Mol. Struct.* **2004**, *703*, 93–101.
- (22) Barthel, J.; Feuerlein, F.; Neuder, R.; Wachter, R. *J. Solution Chem.* **1980**, *9*, 209–219.
- (23) Lemmer, U.; Heun, S.; Mahrt, R. F.; Scherf, U.; Hopmeier, M.; Siegner, U.; Göbel, E. O.; Müllen, K.; Bäessler, H. *Chem. Phys. Lett.* **1995**, *240*, 373–378.
- (24) Knaapila, M.; Almásy, L.; Garamus, V. M.; Pradhan, S.; Pearson, C.; Petty, M. C.; Scherf, U.; Burrows, H. D.; Monkman, A. P. *Macromolecules*, submitted for publication.
- (25) Mukerjee, P.; Mysels, K. J. *Critical Micelle Concentration of Aqueous Surfactant Systems*; National Bureau of Standards: Washington, D.C., 1971.
- (26) Holmberg, K.; Jönsson, B.; Kronberg, B.; Lindman, B. *Surfactants and Polymers in Aqueous Solution*, 2nd ed.; Wiley: Chichester, U.K., 2003.
- (27) Lemmer, U.; Heun, S.; Mahrt, R. F.; Scherf, U.; Hopmeier, M.; Siegner, U.; Göbel, E. O.; Müllen, K.; Bäessler, H. *Chem. Phys. Lett.* **1995**, *240*, 373–378.
- (28) Zeng, G.; Yu, W. L.; Chua, S. J.; Huang, W. *Macromolecules* **2002**, *35*, 6907–6914.
- (29) Romaner, L.; Pogantsch, A.; Scanducci de Freitas, P.; Scherf, U.; Gaal, M.; Zojer, E.; List, E. J. W. *Adv. Funct. Mater.* **2003**, *13*, 597–601.
- (30) Gaal, M.; List, E. J. W.; Scherf, U. *Macromolecules* **2003**, *36*, 4236–4237.
- (31) Beljonne, D.; Pourtois, G.; Silva, C.; Hennebicq, E.; Herz, L. M.; Friend, R. H.; Scholes, G. D.; Setayesh, S.; Müllen, K.; Bredas, J. L. *Proc. Natl. Acad. Sci. U.S.A.* **2002**, *99*, 10982–10987.
- (32) Gamerith, S.; Gadermaier, C.; Scherf, U.; List, E. J. W. *Phys. Status Solidi A* **2004**, *201*, 1132–1151.
- (33) Sims, M.; Bradley, D. D. C.; Ariu, M.; Koeberg, M.; Asimakis, A.; Grell, M.; Lidzey, D. G. *Adv. Funct. Mater.* **2004**, *14*, 765–781.
- (34) Tapia, M. J.; Burrows, H. D.; Arroyo, A.; Pradhan, S.; Scherf, U.; Pinazo, A.; Pérez, L.; Morán, C., to be submitted.
- (35) Burrows, H. D.; Lobo, V. M. M.; Pina, J.; Ramos, M. L.; Seixas de Melo, J.; Valente, A. J. M.; Tapia, M. J.; Pradhan, S.; Scherf, U.; Hintschich, S. I.; Rothe, C.; Monkman, A. P. *Colloids Surf., A*, in press.
- (36) Ribeiro, A. C. F.; Lobo, V. M. M.; Valente, A. J. M.; Azevedo, E. F. G.; Miguel, M. G.; Burrows, H. D. *Colloid Polym. Sci.* **2004**, *283*, 277–283.
- (37) Watkins, A. R. *J. Phys. Chem.* **1974**, *78*, 2555.
- (38) Turro, N. J. *Modern Molecular Photochemistry*; University Science Books: Sausalito, CA, 1991.